Phenomenological study of the process $e^+e^- \to \mu^+\mu^-\nu_l\bar{\nu}_l$ at high energy e^+e^- colliders and measurement of the ZWW and γWW couplings

Gilles Couture*

Département de Physique, Université du Québec à Montréal,
C.P. 8888, Succursal A, Montréal, Québec, Canada H3C 3P8

Stephen Godfrey†

Ottawa-Carleton Institute for Physics,
Department of Physics, Carleton University, Ottawa, Canada K1S 5B6

We perform a detailed study of the process $e^+e^- \to \mu^+\mu^-\nu_l\bar{\nu}_l$ including all contributions. The contributions other than from real gauge boson production lead to a rich phenomenology. We explore the use of the process as a means of precision measurement of the ZWW and γWW vertices. We concentrate on CERN LEP II energies, $\sqrt{s} = 200$ GeV, and energies appropriate to the proposed Next Linear Collider high energy e^+e^- collider with center of mass energies $\sqrt{s} = 500$ and 1 TeV. At 200 GeV, the process offers, at best, a consistency check of other processes being considered at LEP 200. At 500 GeV, the parameters κ_γ, λ_γ, κ_Z, and λ_Z can be measured to about ± 0.1 or better at 95% C.L. while at 1 TeV they can be measured to about ± 0.01. At the high luminosities anticipated at high energy linear colliders precision measurements are likely to be limited by systematic rather than statistical errors.

PACS number(s): 13.10.+q, 12.15.Ji, 14.70.−e

I. INTRODUCTION

There is a growing interest in the physics that can be studied at high energy e^+e^- colliders [1]. High energy e^+e^- colliders offer a cleaner environment than multi-TeV hadron colliders and are therefore expected to allow more quantitative studies of physics at the Fermi scale. Some of the physics topics that have been explored are precision measurement of t-quark properties, searches for new physics, electroweak symmetry breaking, tests of QCD, and precision measurements of the electroweak gauge bosons [2].

At the same time there is a growing appreciation that to realistically assess the physics potential of a specific process one must perform detailed studies of the final-state decay products that will be observed by a detector rather than the massive, short-lived states that we are directly interested in [3–8]. Performing such a study greatly increases the complexity of the analysis as one must include finite width effects of the decaying particles and all the background processes that result in the same final state. On the other hand, this complexity results in a much richer phenomenology which more closely describes what is experimentally observed. In addition, the finite width effects are, in some sense, radiative corrections of order $\Gamma/M \sim \alpha$ which must ultimately be included in a full calculation including radiative corrections [4].

In this paper we present a detailed study of the process $e^+e^- \to \nu\bar{\nu}\mu^+\mu^-$ motivated by our interest in the underlying process $e^+e^- \to \nu_e\bar{\nu}_e Z^0$. Although this process has been studied elsewhere [9, 10], none of the previous calculations have included the decay to final-state fermions with finite width effects and the nonresonant backgrounds. We find that including these contributions adds considerably to the richness of the phenomenology. We then use this process to study the $WW\gamma$ and WWZ^0 couplings.

Although experiments at the CERN LEP-100 e^+e^- collider and the SLAC Linear e^+e^- collider [11] (SLC) have provided stringent tests [12, 13] of the standard model of the electroweak interactions [14] it is mainly the fermion-gauge boson couplings that have been tested and the gauge sector of the standard model remains largely terra incognita. A stringent test of the gauge structure of the standard model is provided by the trilinear gauge vertices (TGV's): the γWW and ZWW vertices. Within the standard model, these couplings are uniquely determined by SU(2)$_L \times$U(1) gauge invariance so that a precise measurement of the vertex poses a severe test of the gauge structure of the theory. If these couplings were observed to have different values than their standard model values, it would indicate the need for physics beyond the standard model.

A problem common to many processes used to study TGV's is that they involve both the $WW\gamma$ and WWZ vertices making it difficult to disentangle the contributions. In this paper we study the sensitivity of the process $e^+e^- \to (Z,\gamma^*)\nu_l\bar{\nu}_l \to \mu^+\mu^-\nu_l\bar{\nu}_l$ to anomalous couplings in the γWW and ZWW vertices. This process

*Electronic address: couture@osiris.phy.uqam.ca
†Electronic address: godfrey@physics.carleton.ca

offers the possibility of studying the ZWW vertex independently of the γWW vertex by imposing appropriate kinematic cuts to select the invariant mass of the $\mu^+\mu^-$ pair. We start with $\sqrt{s} = 200$ GeV appropriate to LEP 200 since this machine will be operational in the relatively near future [15]. We then turn to the proposed e^+e^- colliders [Japan Linear Collider (JLC), Next Linear Collider (NLC), CERN Linear Collider (CLIC)] with possible center-of-mass energies of $\sqrt{s} = 500$ GeV and 1 TeV [1, 16–18]. It is important to mention that we do not include any beamstrahlung radiation effects in our calculation [19]. These effects are very much machine dependent (beam intensity, bunch geometry, etc.) and known to be negligible at 200 GeV, and small at 500 GeV. However, although they can be quite important at 1000 GeV, there has been recent progress in strategies to minimize the effects of beamstrahlung radiation. Interestingly, such high energy colliders offer the possibility of studying the process $e\gamma \to W^-\nu_e$ or $\gamma\gamma \to W^+W^-$ [8, 20]. Both of these processes have been studied in detail and appear very promising.

The outline of this paper is as follows. In the next section we write down the effective Lagrangian we will be studying and the resulting Feynman rule to give our conventions. We also discuss the present constraints on TGV's and expected constraints from future experiments. In Sec. III we examine in detail the process we are interested in; $e^+e^- \to \mu^+\mu^-\nu\bar{\nu}$ and describe the method of calculation. In Sec. IV we present our results for the three energy regimes that we investigated. We summarize our conclusions in Sec. V.

II. THE WWV EFFECTIVE VERTEX

A particularly useful means of probing for physics at high energy scales is to use the language of effective Lagrangians [13, 21]. An effective Lagrangian parametrizes in as model independent a way as possible the low-energy implications of new physics at a much higher scale M. The effective Lagrangian offers a common language so the sensitivity of various experimental observables can be compared in a model-independent way.

There are several different effective Lagrangians in the literature used to describe the trilinear gauge boson vertices (TGV's). They differ in that they make different assumptions on the symmetries and particle content respected by the effective Lagrangian. In our analysis we

use the most general parametrization possible that respects Lorentz invariance, electromagnetic gauge invariance, and CP invariance [22–24]. Because this general Lagrangian hides the SU(2)$\times$ U(1) symmetry observed at present energies and obscures the expected size of its parameters, it has been the object of some criticism in the literature [25]. It is, in fact, equivalent to the alternative SU(2)$\times$ U(1) invariant nonlinearly realized Lagrangian written in the unitary gauge upon suitable field redefinitions [26] and in general one can transform the parameters of one effective Lagrangian to the parameters of another [27]. We choose to use the general Lagrangian in our analysis since it has become the standard parametrization used in phenomenology and therefore makes the comparison of the sensitivity of different observables to the TGV's straightforward.

The most general WWV vertex, satisfying Lorentz invariance, U(1) gauge invariance, and CP conservation allows four free independent parameters κ_γ, λ_γ, κ_Z, and λ_Z when the W bosons couple to essentially massless fermions which effectively results in $\partial_\mu W^\mu = 0$ [22, 23]. We do not consider CP-violating operators in this paper as they are tightly constrained by measurement of the neutron electron dipole moment which constrains the two CP-violating parameters to $|\tilde{\kappa}_\gamma|, |\tilde{\lambda}_\gamma| \lesssim 10^{-4}$ [28]. Therefore, the most general Lorentz and CP-invariant vertex compatible with electromagnetic gauge invariance is commonly parametrized as [22, 23]

$$\mathcal{L}_{WWV} = -ig_V\left\{(W_{\mu\nu}^\dagger W^\mu V^\nu - W_\mu^\dagger V_\nu W^{\mu\nu}) + \kappa_V W_\mu^\dagger W_\nu F^{\mu\nu} - \frac{\lambda_V}{M_W^2}W_{\lambda\mu}^\dagger W_\nu^\mu F^{\nu\lambda}\right\}, \quad (1)$$

where V represents either the photon or the Z^0 and W^μ the W^- fields. As usual, $W_{\mu\nu} = \partial_\mu W_\nu - \partial_\nu W_\mu$ and $F_{\mu\nu} = \partial_\mu V_\nu - \partial_\nu V_\mu$ where V is either the photon or the Z boson, M_W is the W boson mass, and $g_\gamma = e$ and $g_{Z^0} = e\cot\theta_W$. Higher dimension operators would correspond to momentum dependence in the form factors which we ignore. At tree level the standard model requires $\kappa_V = 1$ and $\lambda_V = 0$. Note that the presence of the W-boson mass factor in the λ_V term is $ad\ hoc$ and one could argue that the scale Λ of new physics would be more appropriate. We will conform to the usual parametrization and will not address this issue any further.

The resulting Feynman rule for the WWV vertex is given below with the notation and conventions given in Fig. 1:

$$ig_V\{g_{\alpha\beta}[(1 - \tilde{\lambda}\ k_- \cdot q)k_{+\mu} - (1 - \tilde{\lambda}\ k_+ \cdot q)k_{-\mu}] - g_{\alpha\mu}[(1 - \tilde{\lambda}\ k_- \cdot q)k_{+\beta} - (\kappa - \tilde{\lambda}\ k_+ \cdot k_-)q_\mu]$$

$$-g_{\beta\mu}[(\kappa - \tilde{\lambda}\ k_- \cdot k_+)q_\alpha - (1 - \tilde{\lambda}\ k_+ \cdot q)k_{-\alpha}] + \tilde{\lambda}(k_{+\mu}k_{-\alpha}q_\beta - k_{-\mu}q_\alpha k_{+\beta})\}, \quad (2)$$

where $g_V = e$ for $V = \gamma$ and $e\cot\theta_W$ for $V = Z^0$ and $\tilde{\lambda} = \lambda/M_W^2$.

In the static limit (all particles on mass shell), the parameters λ_γ and κ_γ are related to the anomalous magnetic, and electric quadrupole moments of the W boson

by

$$\mu_W = \frac{e}{2M_W}(1 + \kappa_\gamma + \lambda_\gamma)\ , \quad Q_W = \frac{-e}{2M_W^2}(\kappa_\gamma - \lambda_\gamma)\ ,$$

with similar expressions for the weak moments (i.e., those
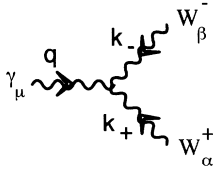
FIG. 1. The trilinear gauge boson vertex.

that involve the Z boson). At tree level, the standard model requires $\kappa_V = 1$ and $\lambda_V = 0$. Higher order corrections to μ_W and Q_W have been calculated in the past and the results are in the 2% range in the minimal standard model and in the 3% range in minimal supersymmetric extensions of the model [29].

Constraints can be obtained from precision measurements on the $WW\gamma$ and WWZ^0 vertices via loop corrections since deviations from their standard model values would have resulted in discrepancies of observables from their standard model predictions [30–32]. At present the limits on TGV's obtained from a global analysis of precision measurements are relatively weak: $|\delta\kappa_\gamma| \leq 0.12$, $|\delta\kappa_Z| \leq 0.08$, $|\lambda_\gamma| \leq 0.07$, and $|\lambda_Z| \leq 0.09$ at 95% C.L. varying one parameter at a time [30]. In a simultaneous fit cancellations could lead to larger values and, in addition, because there are ambiguities in the extraction of these bounds from loop calcuations due to ignorance of the operators values at high energy and the scale of new physics, the bounds obtained in this manner are at best order of magnitude estimates.

In contrast, direct measurements of gauge boson couplings are unambiguous. The only existing direct limits come from the measurement of associated γW production by the UA2 experiment at the CERN $\bar{p}p$ collider which obtained $-3.5 < \kappa_\gamma < 5.9$ and $-3.6 < \lambda_\gamma < 3.5$ at 95% C.L. [33]. The limits obtained from the Fermilab Tevatron are unsettled at present, with two theory analysis finding significantly different limits [34, 35]. The most optimistic limits from the Tevatron are $|\delta\kappa_\gamma| \simeq 3$ and $|\delta\lambda_\gamma| \simeq 1.2$ at 68% C.L. [35]. The sensitivities expected at an upgraded Tevatron with $L = 100$ pb^{-1} are $|\delta\kappa_\gamma| \simeq 1.4$ and $|\delta\lambda_\gamma| \simeq 0.47$ at 90% C.L. [35]. In the near future, the DESY ep collider HERA will be able to constrain the γWW vertex through single W production [36–38] and high p_T photons [39]. Statistics will be the main limiting factor and a precision of ± 0.5 or so is expected [36].

Putting tight constraints on the trilinear gauge boson couplings by studying W pair production is one of the primary motivations for the LEP 200 upgrade [22, 15, 40]. A precision of 30–40 % is expected from a direct measurement of the cross section. If one can reconstruct the W bosons, their angular distribution offers a more sensitive probe and could lead to a bound of 25% or so. Another possibility is to study single W production in $e - \gamma$ collisions [5, 8, 20]. The process $\gamma\gamma \rightarrow W^+W^-$ through heavy ion collisions also offers interesting possibilities [41]. However, one has to deal with an enormous background in the case of head-on collisions or a greatly reduced hard-photon rate for glancing collisions. In the longer term the CERN Large Hadron Collider (LHC) of-

fers good possibilities. Baur and Zeppenfeld [42] have shown that a measurement of $|\delta\kappa_\gamma| \sim 0.2 - 0.5$ at 99.9% C.L. or better is possible, assuming an integrated luminosity of 10^4 pb^{-1}.

In the far future there is growing interest in the physics that can be done at high energy e^+e^- colliders with $\sqrt{s}$ = 500 GeV or $\sqrt{s} = 1$ TeV, referred to as the Next Linear Collider (NLC), the Japan Linear Collider (JLC), or the CERN Linear Collider (CLIC) [1, 16–18]. Various options are being studied including $e\gamma$ collisions where the energetic photons are obtained either by back scattering a laser on one of the incident leptons or by beamstrahlung photons. Measurements at these colliders are very sensitive to anomalous couplings with $e\gamma$ collisions putting some of the more stringent bounds on anomalous $WW\gamma$ couplings [8, 20].

III. CALCULATIONS AND RESULTS

The process $e^+e^- \rightarrow (\gamma^*Z)\nu_l\bar{\nu}_l \rightarrow \mu^+\mu^-\nu_l\bar{\nu}_l$ has several advantages; it is a t-channel process and does not decrease as quickly as s-channel processes as the c.m. energy increases. More importantly, it offers the possibility of isolating the ZWW vertex from the γWW vertex by imposing appropriate cuts on the invariant mass of the $\mu^+\mu^-$ pairs. One drawback is that a total of 28 Feynman diagrams contribute to the process and one has to add incoherently the three families of neutrinos. Although only the two diagrams shown in Fig. 2(a) and 2(b) contribute to the vertex we wish to study, in order to properly take into account the nonresonant backgrounds and maintain gauge invariance, at least in the standard model limit, we must include all 28 diagrams. We leave κ_V and λ_V as free parameters.

To evaluate the cross sections and different distributions we used the CALKUL helicity amplitude technique [43] to obtain expressions for the matrix elements and performed the phase space integration using Monte Carlo techniques [44]. The expressions for the helicity amplitudes are lengthy and unilluminating so we do not include them here. The interested reader can obtain them directly from the authors. To obtain numerical results we used the values $\alpha = 1/128$, $\sin^2\theta = 0.23$, $M_Z = 91.187$ GeV, $\Gamma_Z = 2.5$ GeV, $M_W = 80.2$ GeV, and $\Gamma_W = 2.1$ GeV.

The signal we are studying is an energetic $\mu^+\mu^-$ pair plus missing transverse momentum due to the neutrinos coming from the original beams. In order to eliminate potential background from $e^+e^- \rightarrow e^+e^-\mu^+\mu^-$ via two photons, where the e^+ and e^- escape down the beam pipe, we require missing $\not{p}_T \geq 10$ GeV. We also require $10 \leq E_{\mu^\pm} \leq \sqrt{s}/2 - 10$ GeV, to avoid two-body s-channel processes and box diagrams. Note that these kinematic cuts overlap. In order to take into account finite detector acceptance, we require that the μ^+ and μ^- be at least 10 degrees away from the beam line. Our conclusions are not very sensitive to the exact values of these cuts.

In Fig. 3 we show the cross section for $e^+e^- \rightarrow \nu_l\bar{\nu}_l\mu^+\mu^-$ as a function of $\sqrt{s}$ with the cuts described above and consider the effects of different cuts on the invariant mass of the $\mu^+\mu^-$ pairs. We note that, as ex-

pected of typical t-channel behavior, the cross section does not go down with energy as does the QED point cross section. The cross section for no cuts on $M_{\mu^+\mu^-}$ (solid line) is considerable but it is dominated by low invariant mass events due to the photon pole which appears in many of the Feynman diagrams including photon bremsstrahlung and the diagram of interest in Fig. 2(a). For the most part the low invariant mass contributions are an unwanted background which obscures the physics we are interested in. Imposing a cut of $M_{\mu^+\mu^-} > 25$ GeV eliminates this pole and reduces the cross section substantially (long-dashed line). Finally, if we impose the cut that $M_{\mu^+\mu^-}$ lies within 5 GeV of the Z pole (dotted line) we can separate the effects of the ZWW vertex from the γWW vertex since the photon contribution is now smaller by a factor $(\Gamma_Z/M_Z)^2$. This last curve is in fact the superposition of two diagrams: the s-channel process of Fig. 2(b) which rises sharply above 200 GeV and falls quickly at $\sqrt{s} \geq 300$ GeV and the W fusion

diagrams that fall quickly below 200 GeV and rise up to 1000 GeV. The cut $M_{\mu^+\mu^-} \geq 25$ GeV is an intermediate state between this extreme and the photon-dominated case where the photon bremsstrahlung diagrams dominate for the entire energy range.

It is clear from this figure that this process is hopeless for LEP 100; without any cut on $M_{\mu^+\mu^-}$ the cross section is substantial, but rather insensitive to variations on κ_V and λ_V. Imposing a cut on the invariant mass increases the sensitivity to anomalous couplings but reduces the cross section to an unmeasurable level.

A. $\sqrt{s} = 200$ GeV

For $\sqrt{s} = 200$ GeV we use the kinematic cuts $5 < E_{\mu^\pm} < 95$ GeV and $\not{p}_T > 5$ GeV. The cross section with these cuts and in addition, cuts on $M_{\mu^+\mu^-}$ of no cut, $M_{\mu^+\mu^-} > 10$ GeV, and 86 GeV $< M_{\mu^+\mu^-} < 96$ GeV are 1.9 pb, 0.23 pb, and 0.035 pb, respectively. The latter cut
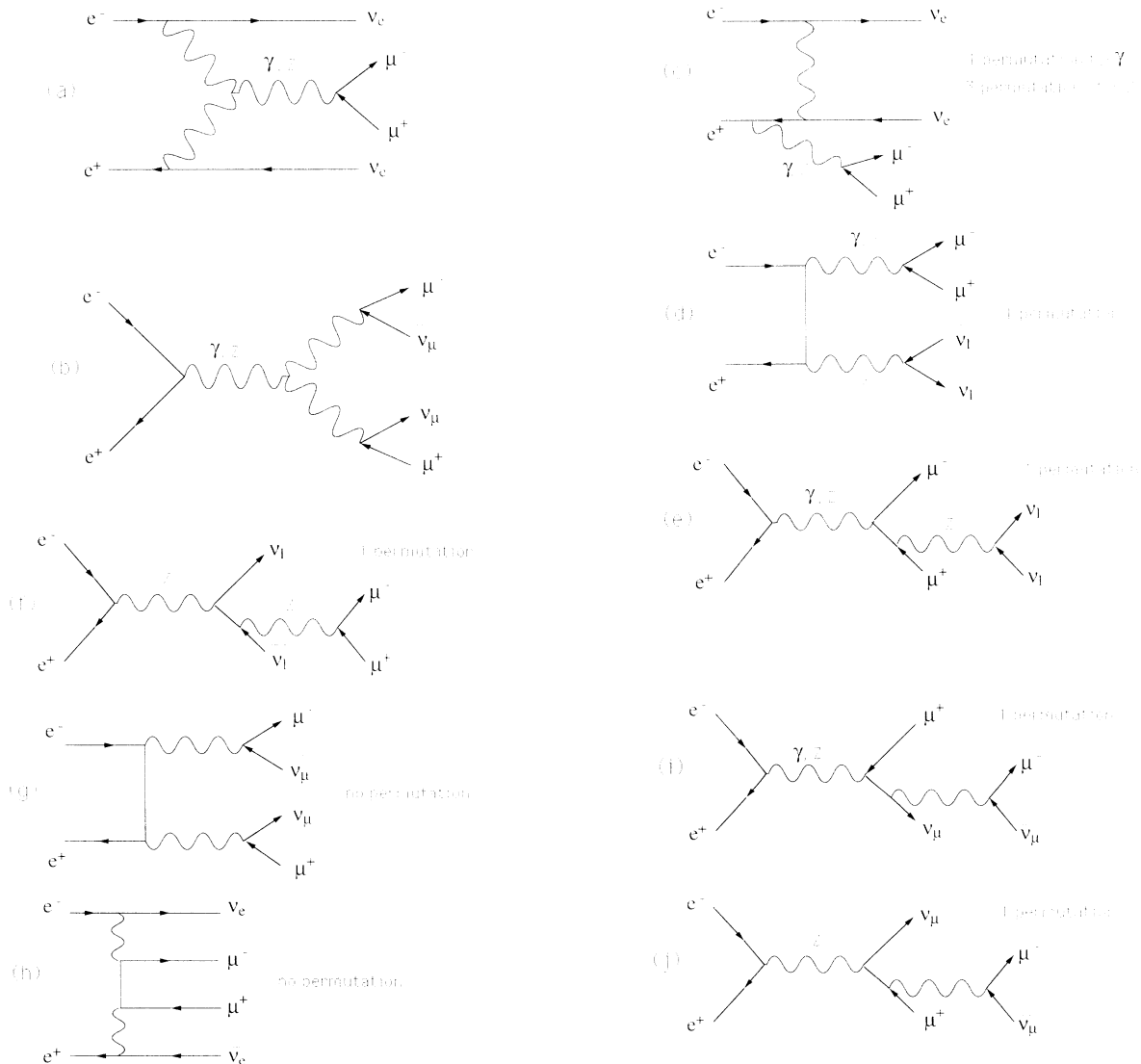

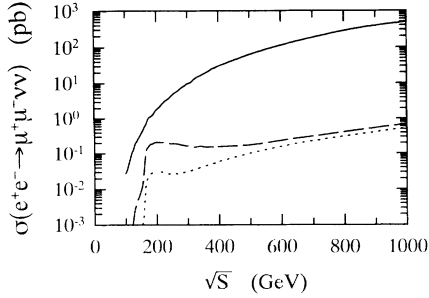FIG. 2. The Feynman diagrams contributing to the process $e^+e^- \to \mu^+\mu^-\nu\bar{\nu}$.

FIG. 3. The cross section $\sigma(e^+e^- \to \mu^+\mu^-\nu\bar\nu)$ as a function of $\sqrt{s}$. The solid line is for the cuts on $E_{\mu\pm}$, $\not\!p_T$, and $\cos\theta_{\mu\pm}$ given in the text. The dashed line adds the cut $M_{\mu^+\mu^-} > 25$ GeV and the dotted line has $|M_{\mu^+\mu^-} - M_Z| < 5$ GeV.

would isolate the effects of the WWZ vertex from that of the $WW\gamma$ vertex. Unfortunately, for the parameters of LEP 200 ($\sqrt{s} = 200$ GeV and an integrated luminosity of 250 pb^{-1}) the number of events remaining after these cuts is not statistically useful.

To maximize the sensitivity to anomalous TGV couplings we examined numerous kinematic distributions. The two which best separated the uninteresting photon bremsstrahlung contribution from signals for anomalous couplings are $d\sigma/dM_{\mu^+\mu^-}$ and $d\sigma/d\cos\theta_{\mu^+\mu^-}$ which are shown in Fig. 4 for several values of κ_γ, λ_γ, κ_Z, and λ_Z, where $\theta_{\mu^+\mu^-}$ is the angle between the μ^+ and μ^-.
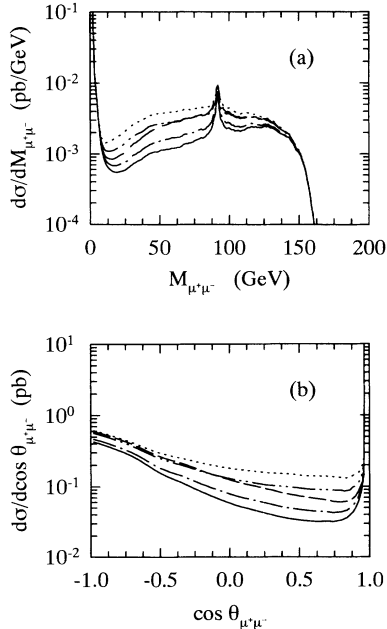

FIG. 4. (a) $d\sigma/dM_{\mu^+\mu^-}$ and (b) $d\sigma/d\cos\theta_{\mu^+\mu^-}$ at $\sqrt{s} = 200$ GeV. In both cases the solid line is for the standard model values of κ_γ, λ_γ, κ_Z, and λ_Z, the long dashed line is for $\delta\kappa_\gamma = \lambda_\gamma = \lambda_Z = 0$ and $\delta\kappa_Z = 2$; the dotted line is for $\delta\kappa_\gamma = \lambda_\gamma = \delta\kappa_Z = 0$; and $\lambda_Z = 2$ the dot-dashed line is for $\delta\kappa_Z = \lambda_\gamma = \lambda_Z = 0$ and $\delta\kappa_\gamma = 2$ and dot-dot-dashed line is for $\delta\kappa_\gamma = \lambda_Z = \delta\kappa_Z = 0$ and $\lambda_\gamma = 2$ where $\delta\kappa_V = \kappa_V - 1$. In this figure and all subsequent ones, the small bumps are due to statistical fluctuations arising from the Monte Carlo phase space integration.

It is clear from Fig. 4(a) that the cross section is most sensitive to anomalous couplings away from the Z^0 resonance which is dominated by W^+W^- production at $\sqrt{s} = 200$ GeV. We therefore examined the effects of removing the contribution of the Z^0 pole; $10 < M_{\mu^+\mu^-} < 88$ GeV. Although this increased the "signal to background" it also reduced the cross section. Once realistic efficiencies are considered we do not feel that enough events would be left to improve the measurement of the TGV's. We included the cuts of $M_{\mu^+\mu^-} > 10$ GeV and $\cos\theta_{\mu^+\mu^-} < 0.95$ in our subsequent calculations used to determine the sensitivity of the measurements to anomalous couplings. We note that these two cuts correspond to the same region in phase space and therefore overlap. In addition, deviations from the standard model show up in various distributions such as $d\sigma/d\cos\theta_{\mu^+\mu^-}$ and we could bin these distributions to perform a χ^2 analysis. In practice, however, the cross section is too small at $\sqrt{s} = 200$ GeV to improve the sensitivity.

Since there are four free parameters, the parameter space is four dimensional which can be projected onto six two-dimensional planes. We performed an extensive search in the parameter space and found that to a good approximation the largest ellipse in any given plane is reached when the other two parameters are kept at their standard model values. The small exception is the relative insensitivity to variations in κ_γ which results in a very small enlargement of the boundary for nonstandard model values along the κ_γ axis. The 95% C.L. for integrated luminosities of 250 pb^{-1} and 500 pb^{-1} for the two planes κ_Z versus λ_Z and κ_γ versus λ_γ are shown in Fig. 5. These bounds represent the regions of the parameter space that can be ruled out as inconsistent with the standard model for a measurement of the standard
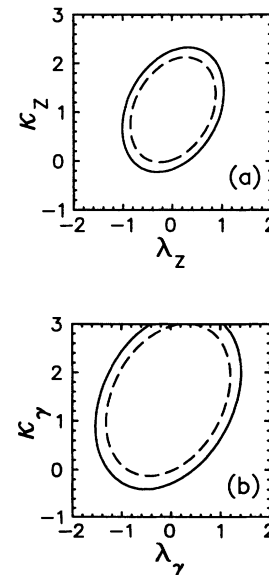

FIG. 5. Sensitivities of the TGV's to anomalous couplings at 95% C.L. based on the kinematic cuts given in the text. The solid lines are based on the statistics assuming an integrated luminosity of 250 pb^{-1} and the dashed lines are based on integrated luminosities of 500 pb^{-1}.

model values for the given integrated luminosity. If we vary one parameter at a time and hold the rest at their standard model values we obtain the limits, based on the statistical error obtained from an integrated luminosity of 500 pb^{-1}, $\delta\kappa_\gamma = {}^{+1.9}_{-1.0}$, $\delta\lambda_\gamma = {}^{+0.9}_{-1.3}$, $\delta\kappa_Z = \pm1.0$, $\delta\lambda_Z = \pm0.8$ at 95% C.L. In this analysis we did not assume any constraints on the parameters. Imposing a custodial SU(2) symmetry gives the relation $\lambda_Z \simeq \lambda_\gamma$ [45]. If we also take $\kappa_Z = \kappa_\gamma$ we obtain the sensitivities $\delta\lambda = {}^{+0.6}_{-0.7}$ and $\delta\kappa = {}^{+1.0}_{-0.6}$ at 95% C.L. which is not so different from the unconstrained result for the Z parameters but significantly tighter than the unconstrained results we obtained for κ_γ and λ_γ. Since the contour axes are almost aligned with the parameter axes two planes contain most, if not all the information about the limits on the four parameters.

At 200 GeV the e^+e^- cross section to four fermions is dominated by W^+W^- production. Note that this dominance does not hold at higher energies where diagram (2h) becomes more and more important. We find that the constraints that can be achieved using the process $e^+e^- \to \mu^+\mu^-\nu\bar\nu$ cannot compete with the constraints obtained from other four fermion final states. In effect, at this center-of-mass energy, we have chosen a final state with a small branching fraction. Therefore, at 200 GeV, this process would provide at best a consistency check for other measurements.

B. $\sqrt{s} = 500$ GeV

We next turn to an "NLC"-type e^+e^- collider with $\sqrt{s} = 500$ GeV. We consider integrated luminosities of 10 and 50 fb^{-1} and use the kinematic cuts 10 GeV $< E_{\mu^\pm} < 240$ GeV and $p_T > 10$ GeV. With these cuts we obtain the invariant mass distribution, $d\sigma/dM_{\mu^+\mu^-}$ shown in Fig. 6.

The increased cross section and expected high luminosity at the NLC leads to a significantly larger number of events making it possible to study the reaction at the Z^0 pole, significantly reducing the contributions of the γWW vertex to the process. Although results have been presented previously for $|M_{\mu^+\mu^-} - M_Z| < 5$ GeV
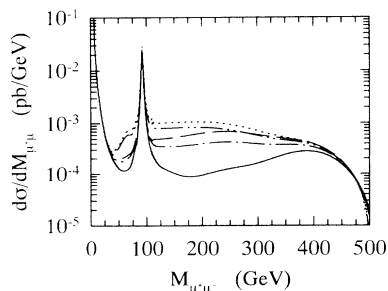
[7] the luminosity that the NLC is expected to achieve is significantly higher than what was used in the earlier analysis. We have therefore revised the analysis taking into account the higher luminosity and emphasizing its implications before proceeding to the results off the Z^0 resonance. In particular we will see that systematic errors will play an increasingly important role in precision measurements.

For the cut $|M_{\mu^+\mu^-} - M_Z| < 5$ GeV we verified that the cross section and distributions are insensitive to variations in κ_γ and λ_γ. We considered the effects of varying κ_Z and λ_Z on the cross section $\sigma(e^+e^- \to \mu^+\mu^-\nu_l\bar\nu_l)$ and found that varying one parameter at a time we obtained a sensitivity (in the sense of consistency with the standard model) of $\delta\kappa_Z = \pm0.1$ ($\lambda_Z = 0$) and $\delta\lambda_Z = {}^{+0.2}_{-0.5}$ ($\kappa_Z = 1$) at 95% C.L. based on 20 fb^{-1} integrated luminosity. However, when we let both parameters vary at the same time we find that regions in the parameter space very far from the standard model give cross sections consistent with the standard model value [7]. To eliminate the ambiguities we examined a number of kinematic distributions. The most sensitive are the angular distribution of the muons with respect to each other ($\theta_{\mu^+\mu^-}$) and the transverse momentum of the reconstructed Z^0 boson (p_{TZ}) which we show in Fig. 7 for several values of κ_Z and λ_Z. We performed a χ^2 analysis based on the angular distribution using the bins; $-1.0 < \theta_{\mu^+\mu^-} < -0.5$, $-0.5 < \theta_{\mu^+\mu^-} - 0.1$, and $-0.1 < \theta_{\mu^+\mu^-} < 0.75$ and another one based on the p_{TZ} distribution with the bins; $p_{TZ} < 80$ GeV, 80 GeV $< p_{TZ} < 120$ GeV, and 120 GeV $< p_{TZ} < 240$ GeV. The 68%, 90%, and 95% C.L. bounds using $d\sigma/d\cos\theta_{\mu^+\mu^-}$ and $d\sigma/dp_{TZ}$ based on 10 fb^{-1} are

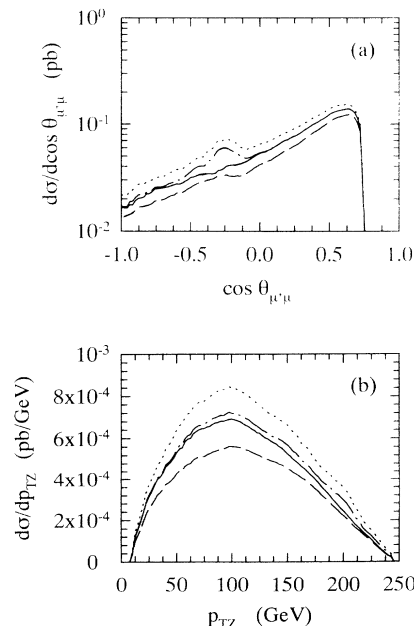FIG. 6. $d\sigma/dM_{\mu^+\mu^-}$ at $\sqrt{s} = 500$ GeV. The solid line is for standard model values of κ_γ, λ_γ, κ_Z, and λ_Z, the long dashed line is for $\delta\kappa_\gamma = \lambda_\gamma = \lambda_Z = 0$ and $\delta\kappa_Z = -0.5$; the dotted line is for $\delta\kappa_\gamma = \lambda_\gamma = \delta\kappa_Z = 0$ and $\lambda_Z = 1$ the dot-dashed line is for $\delta\kappa_Z = \lambda_\gamma = \lambda_Z = 0$ and $\delta\kappa_\gamma = 0.5$ and dot-dot-dashed line is for $\delta\kappa_\gamma = \lambda_Z = \delta\kappa_Z = 0$ and $\lambda_\gamma = 0.5$.

FIG. 7. (a) $d\sigma/d\cos\theta_{\mu^+\mu^-}$ and (b) $d\sigma/dp_{TZ}$ at $\sqrt{s} = 500$ GeV with $|M_{\mu^+\mu^-} - M_Z| < 5$ GeV. In both cases the solid line is for standard model values of κ_γ, λ_γ, κ_Z, and λ_Z, the long dashed line is for $\delta\kappa_\gamma = \lambda_\gamma = \lambda_Z = 0$ and $\delta\kappa_Z = -0.5$; the dotted line is for $\delta\kappa_\gamma = \lambda_\gamma = \delta\kappa_Z = 0$ and $\lambda_Z = 0.5$ and dot-dashed line is for $\delta\kappa_\gamma = \lambda_Z = \delta\kappa_Z = 0$ and $\lambda_\gamma = -0.5$.

shown in Figs. 8(a) and 8(b), respectively. This additional information substantially restricts the allowed region in parameter space that is consistent with the standard model with $\delta\kappa_Z = \pm 0.2$ and $\delta\lambda = {}^{+0.3}_{-0.4}$ at 95% C.L.

These results were based on 10 fb^{-1} of integrated luminosity. It is expected that the luminosity is likely to be higher than this which would improve the measurement capabilities. On the other hand we have neglected systematic errors in our analysis. Monte Carlo studies of SLD-type detectors give very crude estimates of systematic errors of 5% for cross-section measurements [46]. In Fig. 9 we show the 95% C.L. assuming 10 fb^{-1} and 50 fb^{-1} with and without a 5% systematic measurement error. We find that although improving the statistical error improves the sensitivity, the systematic error tends to be more important. In other words, one gains more by reducing the systematic error than by significantly increasing the luminosity.

One might think that the low sensitivity to the WWZ vertex is due to our signal being dominated by the ZZ background of diagrams (2d). By imposing cuts on both the $\mu^+\mu^-$ invariant mass and the recoil missing mass, $M^2_{\rm recoil} = (p_{e^+} + p_{e^-} - p_{\mu^+} - p_{\mu^-})^2$, we can isolate ZZ production. At 500 GeV we find that ZZ production contributes a relatively small amount to the cross section with $M_{\mu^+\mu^-} \simeq M_Z$, while at 1 TeV the ZZ contribution falls to less than a fraction of a percent of the signal. At high energy the Z-bremsstrahlung contributions of diagram (2c) become increasingly important.

Although these results are no improvement over the expected LEP 200 measurements based on W^+W^- pair production, they offer a means of measuring the WWZ vertex independently of the $WW\gamma$ vertex.

Whereas isolating the Z^0 pole offers a means of studying the WWZ vertex independently of the $WW\gamma$ ver-
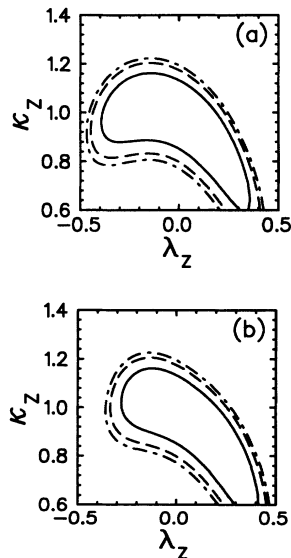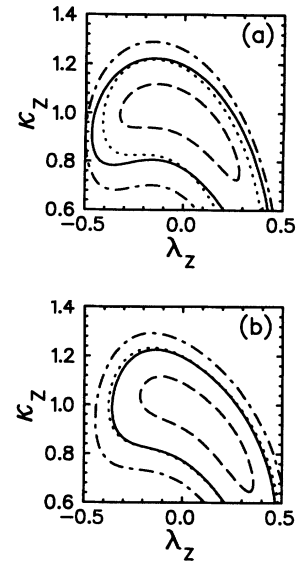

FIG. 9. 95% C.L. bounds of the TGV's based on (a) $d\sigma/d\cos\theta_{\mu^+\mu^-}$, (b) $d\sigma/dp_{T_Z}$ at $\sqrt{s} = 500$ GeV with $|M_{\mu^+\mu^-} - M_Z| < 5$ GeV using the binning given in the text. In both cases the solid curves are based on 10 fb^{-1}, the dashed curves on 50 fb^{-1}, the dot-dashed curves on 10 fb^{-1} + $\delta^{\rm sys}$, and the dotted curves on 50 fb^{-1} + $\delta^{\rm sys}$ where $\delta^{\rm sys}$ =5%.

tex, there is a severe penalty in terms of reduced cross section and sensitivity to anomalous coupling. We therefore examine less restrictive cuts on the $\mu^+\mu^-$ invariant mass which restores the $WW\gamma$ vertex. We searched for the range of $M_{\mu^+\mu^-}$ which exhibited the largest sensitivity to anomalous couplings and found it to be $110 \le M_{\mu^+\mu^-} \le 400$ GeV. As before, with four independent parameters, an extensive search in the parameter space showed that, to a good approximation, the largest (weakest) confidence limit bounds in any two parameters are reached when the other two parameters are kept at their standard model values. The contours for κ_γ vs λ_γ and κ_Z vs λ_Z are shown in Figs. 10(a) and 10(b), respectively, based on the statistics from 10 fb^{-1} integrated luminosity. These bounds were improved slightly when we relaxed the acceptance cuts around the beam axis to $|\cos\theta| < 0.8$ from $10° < \theta < 170°$. We examined other kinematic distributions but found that for the parameter range allowed by Fig. 10, the distributions are very similar and did not offer a significant improvement of the bounds obtained from the cross section measurement. (Imposing the kinematic cuts $E_Z < 300$ GeV gave a very slight improvement and $p_{T_Z} > 100$ GeV distorted the ellipses to give a slight improvement on $\delta\lambda_Z$.)

Finally, we binned the $\mu^+\mu^-$ invariant mass distribution into four bins: $25 < M_{\mu^+\mu^-} < 86$, $86 < M_{\mu^+\mu^-} < 96$, $96 < M_{\mu^+\mu^-} < 110$, and $110 < M_{\mu^+\mu^-} < 400$ and performed a χ^2 analysis, varying one parameter at a time. The resulting 95% C.L. bounds based on $L=10$ fb^{-1} and $L=50$ fb^{-1} with and without systematic errors are summarized in Table I along with our other results for $\sqrt{s} = 500$ GeV. As before, one should be cautious about possible ambiguities when interpreting the results obtained by varying only one parameter at a time. Only

FIG. 8. Sensitivities of the TGV's to anomalous couplings for $\sqrt{s} = 500$ GeV and $L=10$ fb^{-1} based on (a) $d\sigma/d\cos\theta_{\mu^+\mu^-}$ (b) $d\sigma/dp_{T_Z}$ with $|M_{\mu^+\mu^-} - M_Z| < 5$ GeV using the binning given in the text. In both cases the solid lines are 68% C.L., the dashed lines are 90% C.L., and the dot-dashed curves are 95% C.L.
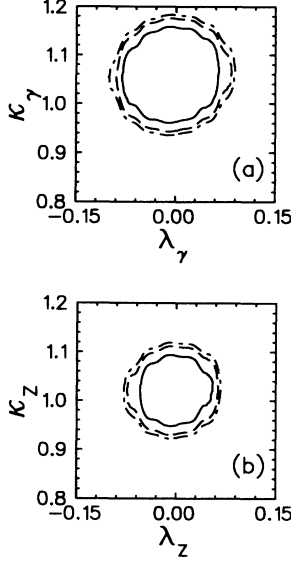
FIG. 10. Sensitivities of the TGV's to anomalous couplings for $\sqrt{s} = 500$ GeV and $L=10$ fb^{-1} based on the total cross section integrated over the kinematic region $110 \leq M_{\mu^+\mu^-} \leq 400$ GeV. The solid lines are 68% C.L., the dashed lines are 90% C.L., and the dot-dashed curves are 95% C.L.

FIG. 11. Sensitivities of the TGV's to anomalous couplings for $\sqrt{s} = 1$ TeV and $L=50$ fb^{-1} based on (a) $d\sigma/d\cos\theta_{\mu^+\mu^-}$, (b) $d\sigma/dp_{T_Z}$ with $|M_{\mu^+\mu^-} - M_Z| < 5$ GeV using the binning given in the text. In both cases the solid lines are 68% C.L., the dashed lines are 90% C.L., and the dot-dashed curves are 95% C.L.

the results for $L=50$ fb^{-1} approach the sensitivity required to observe loop contributions to the TGV's. However, when systematic errors are included it is unlikely that these measurements will reveal nonstandard model physics through radiative corrections to the TGV's. In addition the systematic errors are the limiting factor in the sensitivities, not the statistical errors.
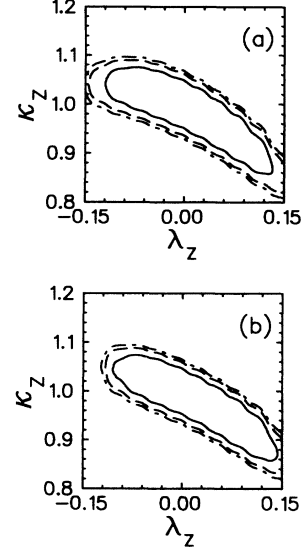
C. $\sqrt{s} = 1$ TeV

The final case we consider is a 1 TeV e^+e^- collider. Although beamstrahlung effects are known to be important in this energy regime [19], we will neglect them since they depend on many machine dependent factors making it difficult to estimate at this time. In any case,

TABLE I. Sensitivities to κ_γ, λ_γ κ_Z, and λ_Z at 95% C.L. from the process $e^+e^- \to \mu^+\mu^-\nu\bar{\nu}$ at a 500 GeV e^+e^- collider. The statistical error is based on the specified integrated luminosity and δ^{sys} refers to the systematic error which we take as 5%.

Based on $\sigma(e^+e^- \to \mu^+\mu^-\nu\bar{\nu})$ with $|M_{\mu^+\mu^-} - M_Z| < 5$ GeV			
	$L=20$ fb^{-1}	$L=50$ fb^{-1}	$L=20$ fb^{-1} $+\delta^{\text{sys}}$	$L=50$ fb^{-1} $+\delta^{\text{sys}}$
$\delta\kappa_Z$	±0.1	±0.06	$+0.25$ -0.30	$+0.24$ -0.28
$\delta\lambda_Z$	$+0.18$ -0.53	$+0.12$ -0.48	$+0.34$ -0.7	$+0.33$ -0.7

Based on $d\sigma/dp_{T_Z}$ with $|M_{\mu^+\mu^-} - M_Z| < 5$ GeV			
$\delta\kappa_Z$	$+0.19$ -0.23	±0.09	$+0.26$ -0.32	$+0.19$ -0.23
$\delta\lambda_Z$	$+0.27$ -0.36	$+0.15$ -0.20	$+0.33$ -0.43	$+0.27$ -0.38

Based on binning $M_{\mu^+\mu^-}$			
	$L=10$ fb^{-1}	$L=50$ fb^{-1}	$L=10$ fb^{-1} $+\delta^{\text{sys}}$	$L=50$ fb^{-1} $+\delta^{\text{sys}}$
$\delta\kappa_Z$	$+0.13$ -0.09	$+0.08$ -0.05	$+0.15$ -0.12	$+0.13$ -0.10
$\delta\lambda_Z$	$+0.082$ -0.090	$+0.055$ -0.060	$+0.096$ -0.107	$+0.082$ -0.090
$\delta\kappa_\gamma$	$+0.21$ -0.09	$+0.17$ -0.05	$+0.27$ -0.11	$+0.21$ -0.08
$\delta\lambda_\gamma$	$+0.09$ -0.12	$+0.06$ -0.07	$+0.12$ -0.14	$+0.09$ -0.12
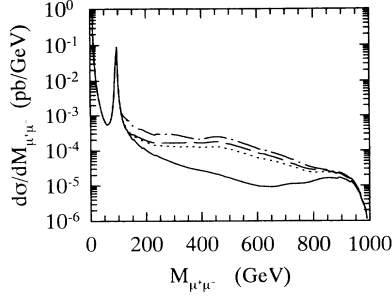
FIG. 12. $d\sigma/dM_{\mu^+\mu^-}$ at $\sqrt{s} = 1$ TeV. The solid line is for standard model values of κ_γ, λ_γ, κ_Z, and λ_Z, the long dashed line is for $\delta\kappa_\gamma = \lambda_\gamma = \lambda_Z = 0$ and $\delta\kappa_Z = -0.2$; the dotted line is for $\delta\kappa_Z = \lambda_\gamma = \lambda_Z = 0$ and $\delta\kappa_\gamma = 0.2$ and dot-dashed line is for $\delta\kappa_\gamma = \lambda_Z = \delta\kappa_Z = 0$ and $\lambda_\gamma = -0.2$.

much progress has been made in understanding how to eliminate beamstrahlung so it may not be as important a factor as originally feared. This should be kept in mind when assessing our results. In what follows we use the kinematic cuts of $p_T > 10$ GeV, $\theta_{\mu\pm} > 10°$, and $10 < E_{\mu\pm} < 490$ GeV.

As before, we imposed a cut on $M_{\mu^+\mu^-}$ to isolate the Z^0WW vertex. The standard model cross section is 0.52 pb. We verified explicitly that varying κ_γ and λ_γ by 10% changed the total cross section by 2 parts in 10 000 or less as expected. Varying κ_Z and λ_Z by 10% changed the total cross section by 2% or less. This small variation does
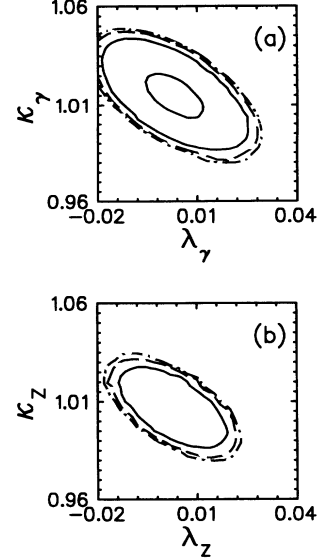

FIG. 13. Sensitivities of the TGV's to anomalous couplings for $\sqrt{s} = 1$ TeV and $L=50$ fb^{-1} based on the total cross section integrated over the kinematic region $200 \le M_{\mu^+\mu^-} \le 900$ GeV. The solid lines are 68% C.L., the dashed lines are 90% C.L., and the dot-dashed curves are 95% C.L.

not translate into particularly significant bounds on the TGV's. As before we performed a χ^2 analysis based on four equal bins for $\theta_{\mu^+\mu^-}$ and the four bins $p_{TZ} < 125$ GeV, 125 GeV $< p_{TZ} < 250$ GeV, 250 GeV $< p_{TZ} < 375$

TABLE II. Sensitivities to κ_γ, λ_γ κ_Z, and λ_Z at 95% C.L. from the process $e^+e^- \to \mu^+\mu^-\nu\bar{\nu}$ at a 1 TeV e^+e^- collider. The statistical error is based on the specified integrated luminosity and δ^{sys} refers to the systematic error which we take as 5%.

	$L=50$ fb^{-1}	$L=200$ fb^{-1}	$L=50$ fb^{-1} $+\delta^{sys}$	$L=200$ fb^{-1} $+\delta^{sys}$
Based on $d\sigma/d\cos\theta_{\mu^+\mu^-}$ with $\|M_{\mu^+\mu^-} - M_Z\| < 5$ GeV				
$\delta\kappa_Z$	± 0.07	± 0.03	$+0.13$ -0.16	$+0.11$ -0.13
$\delta\lambda_Z$	$+0.07$ -0.14	$+0.04$ -0.06	$+0.12$ -0.25	$+0.10$ -0.16
Based on $d\sigma/dp_{TZ}$ with $\|M_{\mu^+\mu^-} - M_Z\| < 5$ GeV				
$\delta\kappa_Z$	± 0.065	± 0.03	$+0.17$ -0.19	$+0.16$ -0.18
$\delta\lambda_Z$	$+0.08$ -0.10	$+0.040$ -0.055	± 0.18	± 0.17
Based on $200 < M_{\mu^+\mu^-} < 900$ GeV				
$\delta\kappa_Z$	$+0.030$ -0.012	$+0.025$ -0.007	$+0.038$ -0.018	$+0.034$ -0.016
$\delta\lambda_Z$	$+0.021$ -0.011	$+0.017$ -0.007	$+0.026$ -0.025	± 0.024
$\delta\kappa_\gamma$	$+0.044$ -0.011	$+0.008$ -0.007	$+0.048$ -0.016	$+0.046$ -0.014
$\delta\lambda_\gamma$	$+0.029$ -0.009	$+0.025$ -0.006	$+0.033$ -0.014	$+0.032$ -0.012
$\delta\kappa_Z$	$+0.030$ -0.012	$+0.025$ -0.007	$+0.038$ -0.018	$+0.034$ -0.016
$\delta\lambda_Z$	$+0.021$ -0.011	$+0.017$ -0.007	$+0.026$ -0.025	± 0.024
$\delta\kappa_\gamma = \delta\kappa_Z$	$+0.027$ -0.006	$+0.006$ -0.003	$+0.033$ -0.009	$+0.032$ -0.008
$\delta\lambda_\gamma = \delta\lambda_Z$	$+0.008$ -0.006	± 0.004	$+0.022$ -0.009	$+0.021$ -0.008

GeV, and $p_{TZ} > 375$ GeV. The 68%, 90%, and 95% C.L. bounds using $d\sigma/d\cos\theta_{\mu^+\mu^-}$ and $d\sigma/dp_{TZ}$ based on 50 fb^{-1} are shown in Figs. 11(a) and 11(b), respectively. Although the TGV's can be constrained to less than about 0.07 with 50 fb^{-1} and less than about 0.04 with 200 fb^{-1}, when a 5% systematic error is included these bounds weaken to about 0.12.

Given these relatively weak bounds we concentrated on a large invariant mass where, although the cross section is reduced, the sensitivity to anomalous coupling is greatly increased. As seen on Fig. 12 the greatest sensitivity to anomalous coupling occurs in the mass range $200 \leq M_{\mu^+\mu^-} \leq 900$ GeV although the upper bound could be pushed to 1 TeV without changing our results. Note that the values used here ($\delta\kappa = \delta\lambda = \pm 0.2$) are extreme and are used simply to illustrate our point. The resulting standard model cross section is 0.024 pb. We show in Fig. 13 two of the six planes of the four-dimensional parameter space. Over this small range in parameter space, the shapes of the different distributions are very similar and one would not gain much (if anything at all) by considering them over a total cross-section measurement. The 95% C.L. bounds that we obtain assuming 50 fb^{-1} and no systematic errors, varying one parameter at a time are $\delta\kappa_\gamma = {}^{+0.04}_{-0.01}$, $\delta\kappa_Z = \pm 0.01$, $\delta\lambda_\gamma = {}^{+0.03}_{-0.01}$, and $\delta\lambda_Z {}^{+0.02}_{-0.01}$. For comparison, the bounds obtained by assuming $\kappa_Z = \kappa_\gamma$ and $\lambda_Z = \lambda_\gamma$ imposed by custodial SU(2) symmetry[1] are slightly stronger with $\delta\kappa = {}^{+0.03}_{-0.006}$ and $\delta\lambda = {}^{+0.008}_{-0.006}$. Again, we emphasize that one must be cautious in interpreting bounds obtained by varying one parameter at a time. The bounds that can be obtained with the various kinematic cuts, luminosities, with and without systematic errors are summarized in Table II. It is clear that the greatly improved sensitivity to anomalous coupling more than compensates for the reduced cross section.

IV. CONCLUSIONS

We have shown that the process $e^+e^- \to \mu^+\mu^-\nu\bar{\nu}$ can be useful in disentangling the different contributions to the γW^+W^- and $Z^0 W^+W^-$ vertices. We included all processes that lead to this four-fermion final state. Ap-

propriate cuts on the invariant mass of the muon pairs offer the possibility of measuring the $Z^0 W^+W^-$ vertex by itself albeit with reduced precision. This is due to both reduced statistics but also due to reduced sensitivity of the process to anomalous couplings. With the cut $|M_{\mu^+\mu^-} - M_Z| < 5$ GeV the cross section is dominated by the one diagram and gauge vertex we are interested in so that there are no sensitive gauge cancellations in the process. On the other hand, off the Z^0 resonance the anomalous couplings can interfere with other diagrams resulting in greater sensitivity to anomalous couplings.

The process turned out to be hopeless at LEP 100 because of the low cross section. At LEP 200 it can lead to, at best, a consistency check of bounds extracted from W-pair production. At higher energy e^+e^- colliders, it can lead to very stringent bounds precise enough to test the TGV's at the level of radiative corrections. The bounds were obtained using many different measurements such as the angular distributions of the outgoing muons, the transverse momentum distribution of the reconstructed Z^0 boson, and the integrated cross section for the process *off* the Z^0 resonance.

Studying the four-fermion final state and including all diagrams which contribute to the final state leads to a much richer phenomenology than would be obtained by simply studying final-state gauge bosons. Thus, the entire process, with all the contributing diagrams, should be studied when examining the physics potential of a specific reaction. We used the high luminosities planned for at the high energy e^+e^- colliders to estimate statistical errors. However, when we included reasonable estimates of systematic errors we found that the limiting factor in high precision measurements will likely be systematic errors not statistical errors. The challenge will therefore be to reduce the systematic errors and one should be very careful with respect to the conclusions one makes by only considering statistical errors.

ACKNOWLEDGMENTS

---

[1] Strictly speaking custodial SU(2) imposes $\lambda_Z = \lambda_\gamma$ and $\kappa_Z = \kappa_\gamma = 1$ [45].

[1] See, for example, B. Wiik, in *Proceedings of the Workshop on Physics and Experiments with Linear e^+e^- Colliders*, Waikoloa Hawaii, 1993, edited by F. Harris (World Scientific, Singapore, 1993), p. 46.

[2] D. Treille, in *Proceedings of the Workshop on Physics and Experiments with Linear e^+e^- Colliders*, [1], p. 1; A. Djouadi and P.M. Zerwas, in Proceedings of *Beyond the Standard Model III*, edited by S. Godfrey and P. Kayniak, Ottawa, Canada, June 1992 (World Scientific, Singapore, 1993), p. 204; A. Miyamoto, in *Proceedings of the Workshop on Physics and Experiments at Linear e^+e^- Colliders*, [1], p. 141.

[3] W. Beenakker and A. Denner, in *Proceedings of the Workshop on Physics and Experiments at Linear e^+e^- Colliders*, [1], p. 704; H. Anlauf, A. Himmler, P. Manakos, T. Mannel, and H. Dahmen, *ibid.*, p. 708; T. Ishikawa *et al.*, KEK Report No. 92-210, 1993 (unpublished).

[4] A. Aeppli, F. Cuypers, and G.J. van Oldenborgh, Paul Scherrer Institut Report No. PSI-PR-93-05 (unpublished).

[5] G. Couture, S. Godfrey, and P. Kalyniak, Phys. Rev D **39**, 3239 (1989); **42**, 1841 (1990); Phys. Lett. **B 218**, 361 (1989), and references therein.

[6] P. Kalyniak, P. Madsen, N. Sinha, and R. Sinha, Phys. Rev. D **48**, 5081 (1993).

[7] G. Couture, S. Godfrey, and R. Lewis, Phys. Rev. D **45**, 777 (1992).

[8] E. Yehudai, Phys. Rev. D **41**, 33 (1990); **44**, 3434 (1991); S. Godfrey and A.K. Peterson, Carleton University Report No. OCIP/C-92-7 (unpublished).

[9] K. Hagiwara et al., Nucl. Phys. **B365**, 544 (1991), and references therein.

[10] S. Ambrosanio and B. Mele, Nucl. Phys. **B374**, 3 (1992).

[11] M. Swartz, Invited talk at the XVI International Symposium on Lepton-Photon Interactions, Cornell University, Ithaca, New York, August 10-15, 1993.

[12] W. Hollik, Invited talk at the XVI International Symposium on Lepton-Photon Interactions, Cornell University [11].

[13] C.P. Burgess, S. Godfrey, H. König, D. London, and I. Maksymyk, this issue, Phys. Rev. D **49**, 6115 (1994).

[14] S.L. Glashow, Nucl. Phys. **22**, 579 (1961); S. Weinberg, Phys. Rev. Lett. **19**, 1264 (1967); A. Salam, in *Elementary Particle Theory: Relativistic Groups and Analyticity (Nobel Symposium No. 8)*, edited by N. Svartholm (Almqvist and Wiksell, Stockholm, 1968).

[15] D. Zeppenfeld, Phys. Lett. B **183**, 380 (1987); D. Treille et al., in *Proceedings of the ECFA Workshop on LEP 200*, Aachen, West Germany, 1986, edited by A. Böhm and W. Hoogland (CERN Report No. 87-08, Geneva, Switzerland, 1987), Vol. 2, p. 414; D.A. Dicus and K. Kallianpur, Phys. Rev. D **32**, 35 (1985); M.J. Duncan and G.L. Kane, Phys. Rev. Lett. **55**, 773 (1985); E.N. Argyres and C.G. Papadopoulos, Phys. Lett. **B263**, 298 (1991).

[16] *Proceedings of the First Workshop on Japan Linear Collider (JLC)*, Tsukuba, Japan, 1989, edited by S. Kawabata (KEK Report No. 90-2, Tsukuba, 1990); *Proceedings of the Second Workshop on Japan Linear Collider*, Tsukuba, Japan, 1990, edited by S. Kawabata (KEK Report No. 91-10, Tsukuba, 1991).

[17] C. Ahn et al., Opportunities and Requirements for Experimentation at a Very High Energy e^+e^- Collider, SLAC Report No. SLAC-0329, 1988 (unpublished).

[18] Proceedings of the Workshop on Physics at Future Accelerators, CERN Yellow Report No. 87-07, 1987 (unpublished).

[19] R. J. Noble, Nucl. Instrum. Methods **A256**, 427 (1987); R. Blankenbecler and S.D. Drell, Phys. Rev. D **36**, 277 (1987); **37**, 3308 (1988); Phys. Rev. Lett. **61**, 2324 (1988); R. Blankenbecler, S.D. Drell, and N. Kroll, Phys. Rev. D **40**, 2462 (1989); D. V. Schroeder, Ph.D. thesis, Stanford, 1990.

[20] S.Y. Choi and F. Schrempp, Phys. Lett. B **272**, 149 (1991).

[21] J. Bagger, *Perspectives in the Standard Model*, Proceedings of the 1991 Theoretical Advanced Study Institute, Boulder, Colorado, edited by R. K. Ellis, C. T. Hill, and J. D. Lykken (World Scientific, Singapore, 1992).

[22] K. Hagiwara et al., Nucl. Phys. **B282**, 253 (1987).

[23] K. Gaemers and G. Gounaris, Z. Phys. C **1**, 259 (1979).

[24] K.-i Hikasa, Phys. Rev. D **33**, 3203 (1986); K. Hagiwara et al., Nucl. Phys. **B282**, 253 (1987); J. Fleischer et al., Z. Phys. C **42**, 409 (1989).

[25] A. De Rújula, M.B. Gavela, P. Hernandez, and E. Massó, Nucl. Phys. **B384**, 3 (1993).

[26] C.P. Burgess and D. London, Phys. Rev. D **48**, 4337

(1993); Phys. Rev. Lett. **69**, 3428 (1992).

[27] A.F. Falk, M. Luke, and E.H. Simmons, Nucl. Phys. **B365**, 523 (1991); D. Zeppenfeld, *Proceedings of the Workshop on Physics and Experiments at Linear e^+e^- Colliders*, [1], p. 695.

[28] W.J. Marciano and A. Queijeiro, Phys. Rev. D **33**, 3449 (1986); F. Boudjema, K. Hagiwara, C. Hamzaoui, and K. Numata, ibid. **43**, 2223 (1991).

[29] G. Couture and J.N. Ng, Z. Phys. C **35**, 65 (1987); G. Couture et al., Phys. Rev. D **38**, 860 (1988); **36**, 859 (1987), and references therein. See also E.N. Argyres et al., Nucl. Phys. **B391**, 23 (1993).

[30] C.P. Burgess, S. Godfrey, H. König, D. London, and I. Maksymyk, Carleton University Report No. OCIP/C-93-7, 1993 (unpublished) (**hepph-9307223**).

[31] K. Hagiwara et al., Phys. Lett. B **283**, 353 (1992).

[32] P. Hernández and F.J. Vegas, Phys. Lett. B **307**, 116 (1993); D. Choudhury, P. Roy, and R. Sinha, Report No. TIFR-TH/93-08 (unpublished).

[33] UA2 Collaboration, J. Alitti et al., Phys. Lett. B **277**, 194 (1992).

[34] M.S. Samuel et al., Phys. Rev. Lett. **67**, 9 (1991); M. Samuel et al., Phys. Rev. D **44**, 2064 (1991).

[35] U. Baur and E. L. Berger, Phys. Rev. D **41**, 1476 (1990), and references therein.

[36] D. Atwood et al., in *High Energy Physics in the 1990's*, Proceedings of the Summer Study, Snowmass, Colorado, 1988, edited by S. Jensen (World Scientific, Singapore, 1989), p. 264; U. Baur and D. Zeppenfeld, Nucl. Phys. **B325**, 253 (1989).

[37] D. Atwood et al., in *Research Directions for the Decade*, Proceedings of the Summer Study, Snowmass, Colorado, 1990, edited by E. L. Berger (World Scientific, Singapore, 1991).

[38] P. Salati and J.C. Wallet, Z. Phys. C **16**, 155 (1982); A.N. Kamal et al., Phys. Rev. D **24**, 2482 (1984); H. Neufeld, Z. Phys. C **17**, 145 (1983); G. Altarelli et al., Nucl. Phys. **B262**, 204 (1985); E. Gabrielli, Mod. Phys. Lett. A **1**, 465 (1986); M. Böhm and A. Rosado, Z. Phys. C **39**, 275 (1988).

[39] S. Godfrey, Z. Phys. C **55**, 619 (1992); U. Baur and M.A. Doncheski, Phys. Rev. D **46**, 1959 (1992); T. Helbig and H. Spiesberger, Nucl. Phys. **B373**, 73 (1992).

[40] G. Kane, J. Vidal, and C.P. Yuan, Phys. Rev. D **39**, 2617 (1990), and references therein.

[41] G. Couture, Phys. Rev. D **44**, 2755 (1991).

[42] U. Baur and D. Zeppenfeld, Nucl. Phys. **B308**, 127 (1988); D. Zeppenfeld and S. Willenbrock, Phys. Rev. D **37**, 1775 (1988); U. Baur and D. Zeppenfeld, Phys. Lett. B **201**, 383 (1988); F. Patore and M. Pepe, in *Proceedings of the ECFA Large Hadron Collider Workshop*, Aachen, Germany, 1990, edited by G. Jarlskog and D. Rein (CERN Report No. 90-10, Geneva, Switzerland, 1990), Vol. II, p. 106; E.N. Argyres et al., Phys. Lett. B **272**, 431 (1991); E.N. Argyres et al., ibid. **280**, 324 (1992); F.K. Diakonos et al., ibid. **303**, 177 (1993).

[43] R. Kleiss and W. J. Stirling, Nucl. Phys. **B262**, 235 (1985); Z. Xu, D.-H. Zhang, and L. Chang, ibid. **291**, 392 (1987).

[44] See, for example, V. Barger and R. Phillips, *Collider Physics* (Addison-Wesley, Don Mills, 1987).

[45] M. Kuroda, F.M. Renard, and D. Schildknecht, Phys. Lett. B **183**, 366 (1987).

[46] T. Barklow (private communication).